New fluid model for the turbulent transport due to the ion temperature gradient

Cite as: Physics of Fluids B: Plasma Physics **5**, 1516 (1993); https://doi.org/10.1063/1.860891
Submitted: 05 October 1992 . Accepted: 26 January 1993 . Published Online: 04 June 1998

Chang-Bae Kim, Wendell Horton, and Satoshi Hamaguchi

New fluid model for the turbulent transport due to the ion temperature gradient

Chang-Bae Kim
Department of Physics, Soong Sil University, Seoul, Korea
Wendell Horton
Institute for Fusion Studies, University of Texas at Austin, Austin, Texas 78712
Satoshi Hamaguchi
IBM Thomas J. Watson Research Center, P. O. Box 218, Yorktown Heights, New York 10598

(Received 5 October 1992; accepted 26 January 1993)

A new set of equations appropriate for the study of the turbulence, due to the ion temperature gradient in the slab in the fluid description, is proposed. This model is similar to many existing models including the one used in the work of Hamaguchi and Horton (HH) [S. Hamaguchi and W. Horton, Phys. Fluids B **2**, 1834 (1990)]. The main difference is that in this model the ion diamagnetic drift contributes to the kinetic energy in the energy balance relation. It is achieved through more complete analysis for the polarization drift due to the finite-Larmor-radius effects. The linear growth rate in the model is found to be smaller and the numerical results show that the heat transport is smaller by an order of magnitude when compared to HH.

I. INTRODUCTION

In this paper we derive a new set of fluid equations in order to study the transport due to the ion temperature gradient (η_i). The importance of the study of the η_i turbulence was raised through the observations in the experiments that better ion confinement is achieved with more peaked density profiles (smaller η_i).[1,2] Many works, theoretical[3–10] as well as experimental,[11,12] have been devoted to solving the energy transport due to the η_i modes. Among them, many models[4,5,8,10] are based on the fluid equations. Recently, however, there is evidence that the nonlinear saturation levels indicated by the fluid models appear to be much larger (by at least an order of magnitude) than the levels predicted by the more sophisticated particle simulations.[13] It is generally believed that the lack of the ion Landau damping in the conventional fluid model contributes to the overestimate of the transport—the linear study shows that the phase velocity of the mode is comparable to the ion thermal speed, which indicates that the Landau damping is actually important. In an effort to bring the saturation level down, recent fluid models incorporate the approximated Landau damping term into the equations.[14]

It appears to us, however, that just including the damping effects into the system may not be enough for the saturation to reach the reduced levels that the particle simulations suggest. This is because the treatment of the finite-Larmor-radius effects through the ion polarization drift $\mathbf{v}_p$ is far from complete in the existing models. Typically, in the derivation of $\mathbf{v}_p$ in Ref. 15, the ion temperature is set to be constant, *not* fluctuating. Due to this assumption one encounters the difficulty in working out the energy conservation property—namely, if one includes the compression $\nabla\cdot\mathbf{v}_p$ due to the polarization drift in the heat equation as well as in the continuity equation, one finds it difficult to work out the usual form of the conservation laws. In order to avoid these untoward points, most models either completely neglect $\nabla\cdot\mathbf{v}_p$ in the heat equation or include only part of $\nabla\cdot\mathbf{v}_p$. Consequently, although the ion diamagnetic drift $\mathbf{v}_d$ is assumed to be of the same order of magnitude as $\mathbf{v}_E$, the $\mathbf{E}\times\mathbf{B}$ drift, the diamagnetic drift does not contribute to the kinetic energy in the conservation law. (In Ref. 16, it is pointed out that the expression of the kinetic energy for the perpendicular velocity, diamagnetic as well as $\mathbf{E}\times\mathbf{B}$, is obtained through the ion polarization drift.)

In this paper, rather than attempting to include the Landau damping effects, we try to put the diamagnetic drift on the equal footing as the $\mathbf{E}\times\mathbf{B}$ drift. This may be achieved through more careful treatment of the compression term $\nabla\cdot\mathbf{v}_p$: For now, suffice it to say that while other fluid models use

$$\nabla\cdot\mathbf{v}_p\approx\nabla\cdot\left[\frac{\hat{\mathbf{b}}}{\omega_c}\times\left(\frac{\partial}{\partial t}+(\mathbf{v}_E+\mathbf{v}_d)\cdot\nabla\right)\mathbf{v}_E\right],$$

in this model we have

$$\nabla\cdot\mathbf{v}_p\approx\nabla\cdot\left[\frac{\hat{\mathbf{b}}}{\omega_c}\times\left(\frac{\partial}{\partial t}+\mathbf{v}_E\cdot\nabla\right)(\mathbf{v}_E+\mathbf{v}_d)\right].$$

Here, ω_c is the ion gyrofrequency and $\hat{\mathbf{b}}$ is the unit vector along the magnetic field. In proper units, one can rewrite

$$\nabla\cdot\mathbf{v}_p=-\left(\frac{\partial}{\partial t}\nabla_\perp^2\varphi+\nabla\cdot[\hat{\mathbf{b}}\cdot(\nabla\psi\times\nabla\nabla)\varphi]\right)$$

and

$$\nabla\cdot\mathbf{v}_p=-\left(\frac{\partial}{\partial t}\nabla_\perp^2\psi+\nabla\cdot[\hat{\mathbf{b}}\cdot(\nabla\varphi\times\nabla\nabla)\psi]\right),$$

respectively, where we define $\psi\doteq\varphi+\tau p$ and $\tau\doteq T_i/T_e$.

After we derive the model equations, we compare the characteristics of the linear stability with those in Ref. 4. The result of the comparison is favorable: The linear growth rate γ is much smaller and γ exhibits a nice feature of peaking at $k_y\rho_s<1$. Then, for the study of the heat transport, we solve the model numerically and compare the results with Ref. 4. The saturation levels are found to be an order of magnitude lower than those in Ref. 4, which is consistent with the linear results. In Sec. II, we briefly introduce the model and we compare the results of the linear study with the work of Hamaguchi and Horton (HH)[4] in Sec. III. In Sec. IV, we present the result of the numerical simulation of one parameter set and compare with HH and in Sec. V, we conclude the work. In the Appendix, the detailed derivation of the model is described.

II. MODEL EQUATIONS

Here, we introduce the equations for the perturbations in dimensionless forms from Eqs. (A10), (A12), and (A14) in the Appendix. Detailed derivations of the model are described in the Appendix. The units that we use are $\rho_s \doteq v_s/\omega_c$ for the perpendicular spatial scale, density-gradient length L_n for the parallel spatial scale, $v_s \doteq (T_e/m)^{1/2}$ for the velocity, $t_s \doteq L_n/v_s$ for the time, the equilibrium ion temperature T_i for the temperature, T_e/e for the electric potential, and the equilibrium particle density n_0 for the density. Here, $-e$ is the charge of the electron. Also, the size of the perturbation is normalized by the expansion parameter (ρ_s/L_n). For example, the electric potential $\varphi' = (\rho_s/L_n)(T_e/e)\varphi$, where φ is the dimensionless potential. The perturbations are denoted without any accent symbols—for example, p stands for the pressure perturbation.

In dimensionless forms, the continuity equation (A10) becomes

$$\frac{\partial}{\partial t}(\varphi - \nabla_\perp^2 \psi) + \frac{\partial \varphi}{\partial y} + \nabla_\parallel v_\parallel - \nabla_\perp \cdot \{\varphi, \nabla_\perp \psi\}_{PB} + \mu_\perp \nabla_\perp^4 \psi = 0, \tag{1}$$

where $\tau \doteq T_i/T_e$ and $\{f,g\}_{PB} \doteq \hat{\mathbf{b}} \cdot (\nabla f \times \nabla g)$, the parallel momentum equation (A12) reduces to

$$\frac{\partial v_\parallel}{\partial t} + \nabla_\parallel \psi + \{\varphi, v_\parallel\}_{PB} - \nu_\perp \nabla_\perp^2 v_\parallel - \nu_\parallel \nabla_\parallel^2 v_\parallel = 0, \tag{2}$$

where $\psi \doteq \varphi + p$, and the pressure equation (A14) changes to

$$\frac{\partial}{\partial t}(p - \tau\Gamma n) + \tau\bar{K}\frac{\partial \varphi}{\partial y} + \{\varphi, (p - \tau\Gamma n)\}_{PB} - \chi_\perp \nabla_\perp^2 p - \chi_\parallel \nabla_\parallel^2 p = 0, \tag{3}$$

where $\bar{K} \doteq K - \Gamma$, $K \doteq \eta_i + 1$, and Γ is the adiabatic gas constant. We assume the electrons are adiabatic and enforce the quasilinearity condition $n = \varphi$. The nonadiabatic response of the electrons are not considered in the present paper and left as a future work. We include the classical dissipations due to the particle collisions with the coefficients $\mu_\perp$, $\nu_\perp$, $\nu_\parallel$, $\chi_\perp$, and $\chi_\parallel$. The perpendicular dissipative terms are obtained through the collisional stress tensor of the Braginskii equations.[17] The coefficients normalized in terms of the present units are given by $\mu_\perp = \tau\delta/4$, $\nu_\perp = (3/10)\tau\delta$, $\chi_\perp = \tau\delta$, where $\delta \doteq (\nu_i/\omega_{ci})(L_n/\rho_s)$ and ν_i is the ion collisional frequency.[18] In the weakly collisional limit $\delta \ll 1$. For the parallel diffusion coefficients, $\nu_\parallel$ and $\chi_\parallel$ are chosen to heuristically model the ion Landau damping as in Ref. 18 and they are quantities of order 1.

For the purpose of comparison, we write down the HH model: for the continuity equation,

$$\frac{\partial}{\partial t}(\varphi - \nabla_\perp^2 \varphi) + (1 + \tau K \nabla_\perp^2)\frac{\partial \varphi}{\partial y} + \nabla_\parallel v_\parallel - \nabla_\perp \cdot \{\varphi, \nabla_\perp \varphi\}_{PB} + \mu_\perp \nabla_\perp^4 \varphi = 0, \tag{4}$$

Eq. (2) for the parallel momentum, and for the pressure,

$$\frac{\partial p}{\partial t} + \tau K \frac{\partial \varphi}{\partial y} - \tau\Gamma\nabla_\parallel v_\parallel + \{\varphi, p\}_{PB} - \chi_\perp \nabla_\perp^2 p - \chi_\parallel \nabla_\parallel^2 p = 0. \tag{5}$$

The differences between Eqs. (1) and (3) and (4) and (5) are attributed to the treatments of the ion polarization drift. HH also neglected $\nabla \cdot \mathbf{v}_p$ in Eq. (5).

It is useful to work out the energy balance for the perturbations: it can be done by multiplying Eqs. (1), (2), and (3) with φ, $v_\parallel$, and $p/\tau\Gamma$, respectively, and by adding the resulting equations. Then, one obtains

$$\frac{\partial \mathscr{E}}{\partial t} = -\left(\frac{K}{\Gamma}\right)\overline{\left(p\frac{\partial \varphi}{\partial y}\right)} + (\text{dissipations}),$$

where $\mathscr{E}$ is the total energy density,

$$\mathscr{E} \doteq \frac{1}{2}\overline{\varphi^2} + \frac{1}{2}\overline{|\nabla(\varphi + p)|^2} + \frac{1}{2}\overline{v_\parallel^2} + \frac{1}{2\tau\Gamma}\overline{p^2}. \tag{6}$$

One notices that the perpendicular kinetic energy density [second term on the right-hand side of Eq. (6)] represents both the $\mathbf{E}\times\mathbf{B}$ and the diamagnetic drift. In contrast, for HH, the total energy density for the perturbation is

$$\mathscr{E} \doteq \frac{1}{2}\overline{\varphi^2} + \frac{1}{2}\overline{|\nabla\varphi|^2} + \frac{1}{2}\overline{v_\parallel^2} + \frac{1}{2\tau\Gamma}\overline{p^2}, \tag{7}$$

counting only the $\mathbf{E}\times\mathbf{B}$ drift.

III. LINEAR STUDY

We, now, study the linear stability of the η_i modes. For the purpose of comparison to other works and for simplicity, we drop out the dissipative terms for the linear analysis. We begin by Fourier transforming in the y direction and time and by setting $\nabla_\parallel = (sx)\partial/\partial y$. From Eqs. (1)–(3), one obtains the eigenvalue equation

$$\frac{\partial^2 \varphi}{\partial x^2} + \left[Q(\tau, \eta_i, s, k_y; \omega) + \left(\frac{s^2}{\omega^2}\right)x^2\right]\varphi = 0, \tag{8}$$

where

$$Q(\tau, \eta_i, s, k_y; \omega) = -k_y^2 - \frac{(\omega - 1)}{[(1 + \Gamma\tau)\omega + \tau\bar{K}]}.$$

In Eq. (8), s is the shear parameter $s = L_n/L_s$ and x denotes the distance from the rational surface. Here, ω is normalized to be the phase velocity in the y direction.

(Frequency divided by k_y.) One can show that Eq. (8) reduces to Eq. (2) of Ref. 7 in the limit of $\Gamma=0$.

Since Eq. (8) is of the type of the Weber equation,[19] one finds the relation

$$Q(\tau,\eta_i,s,k_y;\omega_n)=i(2n+1)s/\omega_n\,,$$

which leads to the quadratic equation of ω_n, and one solves for ω_n as

$$\omega_n=\tfrac{1}{2}[1+(1+\Gamma\tau)k_y^2]^{-1}(\Xi_n\pm\Lambda_n^{1/2}), \qquad (9)$$

where

$$\Xi_n\doteq 1-\tau\bar{K}k_y^2-iS_n(1+\Gamma\tau),$$

$$\Lambda_n\doteq\Xi_n^2-i4S_n\tau[1+(1+\Gamma\tau)k_y^2]\bar{K},$$

$$S_n\doteq(2n+1)s.$$

In order to find the critical value η_{ic} of η_i, we compute the imaginary part of $\Lambda_n^{1/2}$: For ω_n to be positive, i.e., unstable mode, it is required from Eq. (9) that the condition

$$\mathrm{Im}(\Lambda_n^{1/2})>\gamma_c \qquad (10)$$

be satisfied, where $\gamma_c\doteq S_n(1+\Gamma\tau)$. By expressing $\Lambda_n^{1/2}$ as

$$\Lambda_n^{1/2}=a+ib,$$

one finds

$$\Lambda_n=(a^2-b^2)+i2ab.$$

From Eq. (9) one obtains

$$a^2-b^2=(1-\tau\bar{K}k_y^2)^2-\gamma_c^2,$$

$$ab=-S_n\{(1+\Gamma\tau)+\tau\bar{K}[2+(1+\Gamma\tau)k_y^2]\}.$$

Then, b^2 is the root of the equation

$$f(b^2)=b^4+[(1-\tau\bar{K}k_y^2)^2-\gamma_c^2]b^2-S_n^2\{(1+\Gamma\tau)+\tau\bar{K}[2+(1+\Gamma\tau)k_y^2]\}^2.$$

If we denote b_0 as the value of b where the minimum of the function f occurs, i.e., $b_0^2=-\tfrac{1}{2}[(1-\tau\bar{K}k_y^2)^2-\gamma_c^2]$, one finds that

$$\gamma_c^2-b_0^2=\tfrac{1}{2}[(1-\tau\bar{K}k_y^2)^2+\gamma_c^2]>0. \qquad (11)$$

Thus, for the condition (10) to be satisfied one must have $f(\gamma_c^2)<0$. Since it is clear that

$$f(\gamma_c^2)/S_n^2=-4\tau(1+K)[1+(1+\Gamma)k_y^2]\bar{K},$$

one finds $\eta_{ic}=\Gamma-1$.

We compute the mode frequencies and the linear growth rates for the first two lowest-order modes $n=0$, 1. The parameters are $\Gamma=5/3$, $\eta_i=2.48$, $s=0.09$, and $\tau=1.47$. The results are shown in Figs. 1 and 2. The growth rates γ^K peak at $k_y<1$. The mode is propagating in the direction of the ion diamagnetic drift and for large k_y the mode frequency is about the order of the diamagnetic drift frequency.

The results of the linear study are compared to HH. From Eqs. (4), (2), and (5), HH obtain the eigenvalue equation [Eq. (19) in Ref. 4] in our notation,

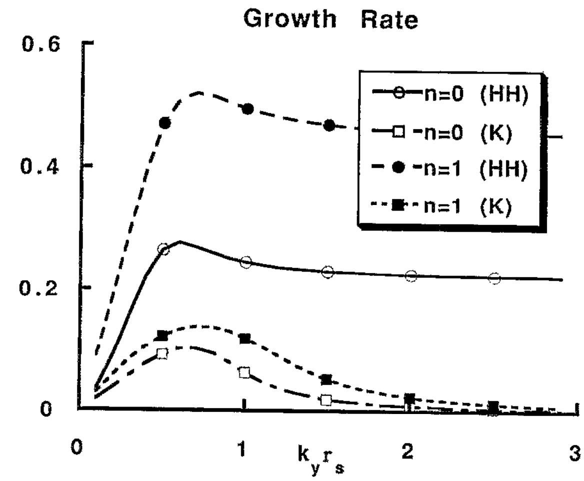

FIG. 1. The linear growth rates of HH and the present work for the first two radial modes: For HH, the solid curve (○) and the short dashed curve (●) are for the modes with the two lowest mode numbers. (In the text, they should correspond to $n=1$ and 2, respectively.) For the present model, the long dashed curve (empty square) and the dotted curve (full square) represent the first two radial modes. In the text, $r_s=\rho_s$. The parameters are $\Gamma=5/3$, $\eta_i=2.48$, $s=0.09$, and $\tau=1.47$.

$$\frac{\partial^2\varphi}{\partial x^2}+\left[Q'+\left(\frac{\omega}{\omega+\tau K}\right)\frac{s^2x^2}{(\omega^2-\Gamma\tau s^2x^2)}\right]\varphi=0, \qquad (12)$$

where

$$Q'=-k_y^2-\left(\frac{\omega-1}{\omega+\tau K}\right).$$

It is useful to transform Eq. (12) to the standard form of the spheroidal wave equation.[19,20] This can be done by transforming $x'=(\Gamma\tau)^{1/2}sx$ and $\varphi=\sqrt{1-x'^2}\varphi'$. Then, up to the leading order, one finds that ω_n satisfies

$$\lambda_n\approx\mu_n+\nu_n\xi_n\,, \qquad (13)$$

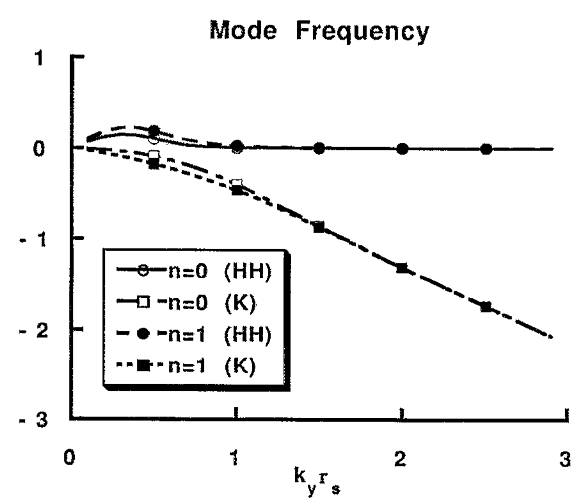

FIG. 2. The mode frequencies of HH and the present work for the first two radial modes: For the symbols and the parameters, see Fig. 1.

where

$$\lambda_n \doteq Q'\left(\frac{\omega_n^2}{s^2\Gamma\tau}\right),$$

$$\zeta_n \doteq \lambda_n - \left(\frac{\omega_n}{\omega_n+\tau K}\right)\left(\frac{\omega_n}{s\Gamma\tau}\right)^2,$$

$$\mu_n = n(n+1),$$

$$\nu_n = \frac{1}{2}\left(1-\frac{3}{(2n-1)(2n+3)}\right).$$

Equation (13) is correct when $\zeta_n < \mathscr{O}(1)$. The cubic equation (13) is solved for two lowest-order modes $n=1$, 2 with the same parameters. The real frequencies and the linear growth rates γ^{HH} are shown in Figs. 1 and 2. The maximum growth rate of HH is about three times larger than the maximum of the present model and γ^{HH} remains finite for large k_y. However, this large-k_y tail decays with the inclusion of the collisional dissipation. Unlike the case with the present model, the mode propagates in the direction of the electron diamagnetic drift.

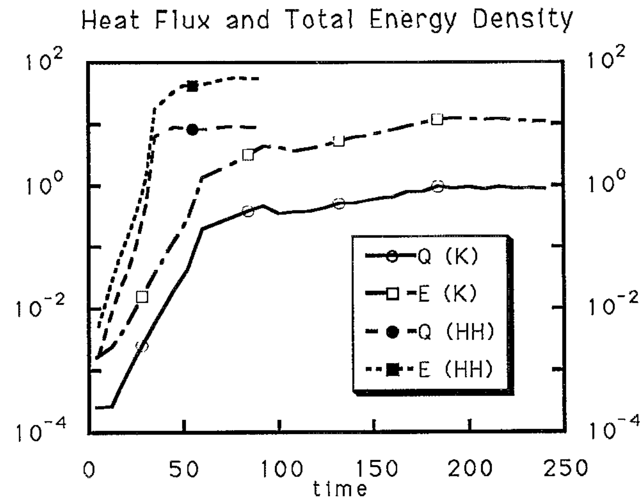

FIG. 3. The comparison of the evolution of the anomalous heat flux Q and the energy density E between the present model (K) and HH. The parameters are $\eta_i=2$, $s=0.1$, $\tau=1$, $\Gamma=2$, $\mu_\perp=\chi_\perp=\nu_\perp=0.01$, and $\chi_\parallel=\nu_\parallel=1.0$. The units are $(\rho_s/Ln^2)(cT_e/eB)$ for Q and $L_n/(T_e/m_i)^{1/2}$ for the time.

IV. NUMERICAL SIMULATIONS

In this section, results of the numerical simulations of the set of equations (1)–(3) are presented and discussed.

The basic structure of the numerical code for the present simulation is the same as the one used in Ref. 4, which is also a modification of the code developed by Park and co-workers.[21,22] With given initial conditions the dependent variables are integrated forward through the predictor–corrector method. The boundary conditions are set so that the perturbations are periodic in y and z directions and vanish far away from the rational surfaces. Thus, one assumes the perturbations as a Fourier sum of the modes traveling along y and z directions and localized in the direction perpendicular to the rational surfaces which lie in the y-z plane. For the simulation, the domain is taken such that $-L_x < x < L_x$, $0<y<L_y$, and $0<z<L_z$ and $L_x=40$, $L_y=10\pi$, and $L_z=7.5\pi$. The boundary condition is forced so that the perturbations vanish at $x=\pm L_x$. Correspondingly, the smallest wave numbers are $(k_y\rho_s)_{\min}=0.2$ and $(k_zL_n)_{\min}=0.27$. As for the number of modes, various numbers of modes are considered and the typical modes used for the data are $0<m<7$ and $-2<n<2$, where $m \doteq k_yL_y/2\pi$ and $n \doteq k_zL_z/2\pi$. The typical values of m and n are chosen such that the inclusion of more modes does not change the result considerably. Since the rational surface of the (m,n) mode locates at $x=(L_y/sL_z)(n/m)$, with the shear parameter $s=0.1$ there are two rational surfaces farthest away from $x=0$ located at $x=\pm 27\rho_s$ and 21 other rational surfaces in between. Consequently, many modes are overlapped around $x=0$. Practically, $L_x=40$ is chosen so that the mode $(m=2,n)$ vanishes smoothly at $x=\pm L_x$. The number of evenly spaced mesh points is 600 and the other parameters used for the simulation are $\eta_i=2$, $s=0.1$, $\tau=1$, $\Gamma=2$, $\mu_\perp=\chi_\perp=\nu_\perp=0.01$, and $\chi_\parallel=\nu_\parallel=1.0$. It is noted from the run that a different choice of small diffusion parameters $\mu_\perp$, $\chi_\perp$, and $\nu_\perp$ does not change the overall result.

With the above parameters and the same initial conditions, the numerical simulations are performed for two models, the present one and HH. Both cases are found to saturate in time although HH reaches the saturation faster than the present model. The mode width in x and y are found to be about two to three times ρ_s. At the saturation, the volume-averaged anomalous heat flux $Q \doteq \overline{\langle p v_x\rangle} = \overline{\langle p\partial\varphi/\partial y\rangle}$ and the energy density $\mathscr{E}$ are computed for both cases. It is found that the present model predicts the saturation levels of both the total energy density and the heat flux about an order of magnitude smaller than HH. The results are shown in Fig. 3. In this run, the background ion pressure gradient is kept constant for both cases in order that the saturation is achieved due to the turbulence rather than due to the quasilinear flattening. The corresponding thermal diffusivity χ_i is computed as follows:

$$\chi_i = \left(\frac{\overline{\langle p_i v_r\rangle}}{-p_{i0}'}\right)_{\text{real units}} = \left(\frac{\overline{\langle p\partial\varphi/\partial y\rangle}}{(1+\eta_i)}\right)_{\text{dimensionless}} \times \frac{\rho_s}{Ln}\frac{cT_e}{eB}. \quad (14)$$

For the present model, from Fig. 3 the dimensionless value $\overline{\langle p\partial\varphi/\partial y\rangle} \approx 1$ [$Q(K)$ in the figure] and $\eta_i=2$, one obtains

$$\chi_i^K \approx 0.3(\rho_s/Ln)(cT_e/eB)$$

and, for the HH model, the dimensionless value $\overline{\langle p\partial\varphi/\partial y\rangle} \approx 10$ [$Q(\text{HH})$ in the figure]

$$\chi_i^{\rm HH} \approx 3.0(\rho_s/Ln)(cT_e/eB),$$

which is ten times higher than χ_i^K.

V. CONCLUSIONS

A new fluid model is proposed for the turbulence due to the ion-temperature gradient. In many respects this model is similar to many existing models. Yet, it encompasses more complete treatment of the ion polarization drift which plays a significant role in developing the instability. Linear study shows that the growth rate for the instability is not so large as other models suggest and consequently the nonlinear saturation is achieved at relatively lower level, about an order of magnitude lower than that of the model HH considered. Specifically, with typical experimental parameters, the new model predicts the thermal diffusivity $\chi_i \approx 0.3(\rho_s/Ln)(cT_e/eB)$ and HH leads to a value about ten times higher. Thus, the present model serves as a better possible alternative to the more complicated particle simulations which suggest that the actual transport due to the ion-temperature gradient be at least an order of magnitude lower than the results of the existing fluid models.

Although the model has good features, it needs to be improved in order to be a more realistic model. One needs to include the Landau damping more physically in the model. Heuristically, the Landau damping is present as the terms represented by $\chi_\parallel$ and $\nu_\parallel$ in the model. One may do better by following the recent works of Hammett,[14] for example. Also, one needs to investigate the effect of the anisotropic nature of the plasma and needs to extend the model to the toroidal geometry.

After this work was completed, it was brought to our attention that the similar equation for the polarization drift was worked out by Chang.[23]

ACKNOWLEDGMENTS

The author is grateful to Dr. J. H. Han for supplying the numerical code to check the eigenvalues.

This work was partially supported by U.S. Department of Energy Contract No. DE-FG05-80ET53088.

APPENDIX: DERIVATIONS OF THE MODEL

Here, we derive the model equations suitable for the transport study at the spatial scale of the ion gyroradius and at the temporal scale of the time for the ions to move a distance of the density gradient length L_n along the magnetic field. This has been achieved in many previous works through the perturbation expansion of the perpendicular velocity in terms of such small parameters as $\epsilon = \rho/L_n$, $[\omega_c(\partial/\partial t)]^{-1}$. We define the gyrofrequency $\omega_c \doteq (qB/mc)$. For the sake of the ordering, it is assumed that the relative sizes of the spatial and the time scales for the perturbations to those of the equilibrium quantities are ϵ. Also, the relative size of the perturbation to the equilibrium quantity is of the order of ϵ.

From the perpendicular momentum equation, one can obtain the balance of the leading-order forces:

$$nq\left(\mathbf{E}+\frac{v}{c}\times\mathbf{B}\right)-\nabla p-\nabla\cdot\Pi^f\approx 0, \tag{A1}$$

where Π^f is the collisionless viscosity tensor due to the finite-Larmor-radius effects. If the magnetic drifts are neglected, the divergence of the tensor is

$$\begin{aligned}\nabla\cdot\Pi^f=&\nabla\cdot\left[\left(\frac{p}{2\omega_c}\right)\nabla_\perp(\hat{\mathbf{b}}\times\mathbf{v})\right]\\&+\nabla_\parallel\left[\left(\frac{p}{\omega_c}\right)\underline{[2\nabla_\parallel(\hat{\mathbf{b}}\times\mathbf{v})-\nabla\times\mathbf{v}]}\right]\\&-\left\{\hat{\mathbf{b}}\cdot\left[\nabla\left(\frac{p}{\omega_c}\right)\times\nabla\right]\right\}\left(\frac{1}{2}\mathbf{v}_\perp+\mathbf{v}_\parallel\right)\\&\underline{-\hat{\mathbf{b}}\left\{\hat{\mathbf{b}}\cdot\left[\nabla\left(\frac{p}{\omega_c}\right)\times\nabla_\parallel\mathbf{v}\right]\right\}}.\end{aligned} \tag{A2}$$

Up to the two leading orders, one can simplify Eq. (A2) to

$$\nabla\cdot\Pi^f\approx\nabla\cdot\Pi_1^f+\nabla\cdot\Pi_2^f, \tag{A3}$$

and

$$\nabla\cdot\Pi_1^f\doteq\left(\frac{p}{2\omega_c}\right)\hat{\mathbf{b}}\times\nabla_\perp^2 v,$$

$$\begin{aligned}\nabla\cdot\Pi_2^f\doteq&\frac{1}{2}\nabla_\perp\left(\frac{p}{\omega_c}\right)\cdot\nabla_\perp(\hat{\mathbf{b}}\times\mathbf{v})+\left(\frac{p}{\omega_c}\right)\hat{\mathbf{b}}\times\nabla(\nabla_\parallel v_\parallel)\\&-\hat{\mathbf{b}}\left(\frac{p}{\omega_c}\right)\nabla_\parallel(\hat{\mathbf{b}}\cdot\nabla\times\mathbf{v})-mn(\mathbf{v}_d\cdot\nabla)\\&\times\left(\frac{1}{2}\mathbf{v}_\perp+\mathbf{v}_\parallel\right),\end{aligned}$$

where the underlined terms in Eq. (A2) are neglected because $|\nabla_\perp|\gg|\nabla_\parallel|$ and $(\nabla\times\mathbf{v})_\perp\approx-\hat{\mathbf{b}}\times\nabla v_\parallel$. In Eq. (A3), the first term on the right-hand side is the leading-order term and $\mathbf{v}_d\doteq(c/nqB)\hat{\mathbf{b}}\times\nabla p$ is the diamagnetic drift. Then, one finds the dominant perpendicular velocity

$$\begin{aligned}\mathbf{v}_\perp&\approx\left(\frac{c}{B}\right)\mathbf{E}\times\hat{\mathbf{b}}_0+\mathbf{v}_d+\left(\frac{cT}{2qB\omega_c}\right)\hat{\mathbf{b}}\times(\hat{\mathbf{b}}\times\nabla_\perp^2\mathbf{v}_\perp),\\&=\mathbf{v}_E+\mathbf{v}_d-\tfrac{1}{2}\rho^2\nabla_\perp^2\mathbf{v}_\perp.\end{aligned}$$

Hence,

$$(1+\tfrac{1}{2}\rho^2\nabla_\perp^2)\mathbf{v}_\perp=\mathbf{v}_E+\mathbf{v}_d.$$

If $|\rho^2\nabla_\perp^2|<1$, then

$$\mathbf{v}_\perp\approx\mathbf{v}_\perp^{(1)}+\mathbf{v}_f, \tag{A4}$$

where

$$\mathbf{v}_\perp^{(1)}\doteq\mathbf{v}_E+\mathbf{v}_d,$$

$$\mathbf{v}_f\doteq(1-\tfrac{1}{2}\rho^2\nabla_\perp^2)\mathbf{v}_\perp^{(1)}.$$

In the following, we will include $\mathbf{v}_f$ only in the expression of $\nabla\cdot\mathbf{v}$ of the continuity equation and the pressure equation because the order of the term $\nabla\cdot\mathbf{v}$ becomes higher as $\nabla\cdot\mathbf{v}_E=\nabla\cdot(n\mathbf{v}_d)=0$ in the slab.

1. Divergence of the polarization drift

As the term $\nabla\cdot\mathbf{v}$ in the continuity equation is of higher order, one needs to consider the higher-order velocity rather than the $\mathbf{E}\times\mathbf{B}$ and the diamagnetic drifts, which is the polarization drift $\mathbf{v}_p$,

$$\mathbf{v}_p \doteq \omega_c^{-1}\hat{\mathbf{b}}_0\times\left[\left(\frac{\partial}{\partial t}+\mathbf{v}_\perp^{(1)}\cdot\nabla\right)\mathbf{v}_\perp^{(1)}+\frac{1}{mn}\nabla\cdot\Pi^f\right],$$

and is the result of the finite-Larmor-radius effects.

After doing a little algebra and by using the identity

$$\nabla\times\left(\frac{\hat{\mathbf{b}}}{B}(\mathbf{v}_E\cdot\nabla p)\right)=-\frac{\hat{\mathbf{b}}}{B}\times\nabla(\mathbf{v}_E\cdot\nabla p)+\left(\frac{q}{cT}\right)(\mathbf{v}_E\cdot\nabla p)\mathbf{v}_g,$$

one finds that

$$\frac{D\mathbf{v}_d}{Dt}=\left(\frac{c}{nqB}\right)\hat{\mathbf{b}}\times\nabla\frac{D^Ep}{Dt}+(\mathbf{v}_d\cdot\nabla)\mathbf{v}_\perp^{(1)}$$
$$\underline{-\frac{1}{n}\left(\frac{\partial n}{\partial t}+\nabla\cdot(n\mathbf{v}_E)\right)\mathbf{v}_d}+\underline{\left(\frac{\nabla p}{p}\right)\times(\mathbf{v}_E\times\mathbf{v}_g)}, \tag{A5}$$

where

$$\frac{D}{Dt}\doteq\frac{\partial}{\partial t}+\mathbf{v}_\perp^{(1)}\cdot\nabla,$$

$$\frac{D^E}{Dt}\doteq\frac{\partial}{\partial t}+\mathbf{v}_E\cdot\nabla=\frac{\partial}{\partial t}+\left(\frac{c}{B}\right)\{\varphi,\cdot\}_{PB},$$

$$\{f,g\}_{PB}\doteq\hat{\mathbf{b}}\cdot(\nabla f\times\nabla g).$$

The underlined terms in Eq. (A5) are smaller than the first term on the right-hand side by an order of magnitude and can be neglected. In most previous works, the first term on the right-hand side in Eq. (A5) is set to be *zero*, which is certainly *not* quite consistent with the heat equation. It turns out later that this term leads to the inclusion of the diamagnetic drift in the kinetic energy density.

By combining Eqs. (A3) and (A5), one obtains

$$mn\frac{D\mathbf{v}_d}{Dt}+(\nabla\cdot\Pi^f)_\perp=\frac{\hat{\mathbf{b}}}{\omega_c}\times\nabla\frac{D^Ep}{Dt}-\nabla_\perp\left[\left(\frac{p}{2\omega_c}\right)\hat{\mathbf{b}}\cdot(\nabla\times\mathbf{v})\right]$$
$$+\underline{\left(\frac{p}{\omega_c}\right)\hat{\mathbf{b}}\times\nabla_\perp(\nabla_\parallel v_\parallel)}$$
$$+\underline{\hat{\mathbf{b}}\times\nabla\left[\left(\frac{p}{2\omega_c}\right)(\nabla\cdot\mathbf{v}_\perp)\right]}. \tag{A6}$$

Upon dropping the underlined terms in Eq. (A6) because they are small if $|\rho^2\nabla_\perp^2|<1$, one obtains

$$\nabla\cdot\left[\frac{\hat{\mathbf{b}}}{\omega_c}\times\left(\frac{D\mathbf{v}_d}{Dt}+\frac{1}{mn}(\nabla\cdot\Pi^f)_\perp\right)\right]\approx\left(\frac{p}{mn\omega_c^2}\right)\nabla_\perp^2\left(\frac{1}{p}\frac{D^Ep}{Dt}\right). \tag{A7}$$

Following, similar steps for the $\mathbf{E}\times\mathbf{B}$ drift, one finds that

$$\nabla\cdot\left(\frac{\hat{\mathbf{b}}}{\omega_c}\times\frac{D\mathbf{v}_E}{Dt}\right)=-\left(\frac{c}{\omega_cB}\right)\left[\frac{\partial}{\partial t}\nabla_\perp^2\varphi\right.$$
$$\left.+\left(\frac{c}{B}\right)\nabla\cdot\left\{\left(\varphi+\frac{p}{nq}\right),\nabla_\perp\varphi\right\}_{PB}\right] \tag{A8}$$

and upon adding Eqs. (A8) and (A7),

$$\nabla\cdot\mathbf{v}_p\approx-\left(\frac{c}{\omega_cB}\right)\left[\frac{\partial}{\partial t}\nabla_\perp^2\left(\varphi+\frac{p}{nq}\right)\right.$$
$$\left.+\left(\frac{c}{B}\right)\nabla\cdot\left\{\varphi,\nabla_\perp\left(\varphi+\frac{p}{nq}\right)\right\}_{PB}\right]. \tag{A9}$$

Again, in the previous derivations, the divergence of the polarization drift is the right-hand side of Eq. (A8) because the right-hand side of Eq. (A7) vanishes.

2. Fluid equations

Upon including the polarization drift, the continuity equation becomes

$$\frac{\partial n}{\partial t}+\mathbf{v}_E\cdot\nabla n+n\nabla\cdot(\mathbf{v}_p+\mathbf{v}_f+v_\parallel\hat{\mathbf{b}})=0. \tag{A10}$$

Now, we show that the convective derivative term $\mathbf{v}_d\cdot\nabla v_\parallel$ in the parallel momentum equation is canceled out by the finite-Larmor-radius viscosity tensor: from Eq. (A2),

$$(\nabla\cdot\Pi^f)_\parallel=-\nabla_\parallel\left[\left(\frac{p}{\omega_c}\right)\hat{\mathbf{b}}\cdot\nabla\times\mathbf{v}_\perp^{(1)}\right]-\hat{\mathbf{b}}\cdot\left[\nabla\left(\frac{p}{\omega_c}\right)\times\nabla v_\parallel\right]$$
$$\underline{-\hat{\mathbf{b}}\cdot\left[\nabla\left(\frac{p}{\omega_c}\right)\times\nabla_\parallel\mathbf{v}_\perp^{(1)}\right]},$$
$$\approx-\left(\frac{c}{B}\right)\left(\frac{p}{\omega_c}\right)\nabla_\parallel\nabla_\perp^2\left(\varphi+\frac{p}{nq}\right)-mn\mathbf{v}_d\cdot\nabla v_\parallel, \tag{A11}$$

where the underlined term is neglected because it has a gradient of (p/ω_c). The first term in Eq. (A11) can also be neglected in the case when $|\rho^2\nabla_\perp^2|<1$. Thus, the equation for the parallel momentum becomes

$$mn\left(\frac{\partial}{\partial t}+\mathbf{v}_E\cdot\nabla\right)v_\parallel=-\nabla_\parallel(nq\varphi+p). \tag{A12}$$

As for the heat equation, we replace the $\nabla\cdot\mathbf{v}$ term with the continuity equation:

$$\nabla\cdot\mathbf{v}\approx\nabla\cdot(\mathbf{v}_\perp^{(1)}+\mathbf{v}_p+\mathbf{v}_\parallel),$$
$$=\nabla\cdot(\mathbf{v}_E+\mathbf{v}_p+\mathbf{v}_\parallel)+\frac{1}{p}\nabla\cdot(p\mathbf{v}_d),$$
$$=-\frac{1}{n}\left(\frac{\partial n}{\partial t}+(\mathbf{v}_E+\mathbf{v}_p+\mathbf{v}_\parallel)\cdot\nabla n\right)+\frac{1}{n}\nabla\cdot(n\mathbf{v}_d)$$
$$+\frac{1}{p}\nabla\cdot(p\mathbf{v}_d),$$

since $|\mathbf{v}_E| \gg |\mathbf{v}_p|$, $|\nabla_\perp| \gg |\nabla_\parallel|$, and $\nabla\cdot(n\mathbf{v}_d)=0$ in the slab,

$$\approx -\frac{1}{n}\left(\frac{\partial n}{\partial t}+\mathbf{v}_E\cdot\nabla n\right)+\frac{1}{p}\nabla\cdot(p\mathbf{v}_d), \qquad \text{(A13)}$$

and the last term $\nabla\cdot(p\mathbf{v}_d)$ will be canceled out in the pressure equation due to the finite-Larmor-radius heat flux. It is important to notice that by using the continuity equation in the place of $\nabla\cdot\mathbf{v}$ one includes the polarization drift consistently in the pressure equation while the previous works do not consider the polarization drift in the equation. One is, thus, led to the equation for the pressure

$$\left(\frac{\partial}{\partial t}+\mathbf{v}_E\cdot\nabla\right)p-\Gamma T_i\left(\frac{\partial}{\partial t}+\mathbf{v}_E\cdot\nabla\right)n=0. \qquad \text{(A14)}$$

[1]M. Greenwald, D. Q. Winn, S. Milora, R. Parker, and S. Wolfe, Phys. Rev. Lett. **53**, 352 (1984).

[2]F. X. Söldner, E. R. Müller, F. Wagner, H. S. Bosch, A. Eberhagen, H. U. Fahrbach, G. Fussmann, O. Gehre, K. Gentle, J. Gernhardt, O. Gruber, W. Herrmann, G. Janeschitz, M. Kornherr, K. Krieger, H. M. Mayer, K. McCormick, H. D. Murmann, J. Neuhauser, R. Nolte, W. Poschenrieder, H. Röhr, K.-H. Steuer, U. Stroth, N. Tsois, and H. Verbeek, Phys. Rev. Lett. **61**, 1105 (1988).

[3]B. Coppi, M. N. Rosenbluth, and R. Z. Sagdeev, Phys. Fluids **10**, 582 (1967).

[4]S. Hamaguchi and W. Horton, Phys. Fluids B **2**, 1834 (1990).

[5]W. Horton, R. D. Estes, and D. Biskamp, Plasma Phys. **22**, 663 (1980).

[6]W. Horton, Phys. Rep. **192**, 177 (1990).

[7]T. S. Hahm and W. M. Tang, Phys. Fluids B **1**, 1185 (1989).

[8]G. S. Lee and P. H. Diamond, Phys. Fluids **29**, 3991 (1986).

[9]N. Mattor and P. H. Diamond, Phys. Fluids B **1**, 1980 (1989).

[10]J. W. Connor, Nucl. Fusion **26**, 193 (1986).

[11]S. D. Scott, P. H. Diamond, R. J. Fonck, R. J. Goldston, R. B. Howell, K. P. Jaehnig, G. Schilling, E. J. Synakowski, M. C. Zarnstorff, C. E. Busch, E. Fredrickson, K. W. Hill, A. C. Janos, D. K. Mansfield, D. K. Owens, H. Park, G. Pautasso, A. T. Ramsey, J. Schivell, G. D. Tait, W. M. Tang, and G. Taylor, Phys. Rev. Lett. **64**, 531 (1990).

[12]M. C. Zarnstorff, C. W. Barnes, P. C. Efthimion, G. Hammett, W. Horton, R. Hulse, D. Mansfield, E. Marmar, K. McGuire, G. Rewoldt, B. Stratton, E. J. Synakowski, W. Tang, J. Terry, X. Q. Xu, M. G. Bell, M. Bitter, N. L. Bretz, R. Budny, C. E. Busch, R. J. Fonck, E. Fredrickson, H. P. Furth, R. J. Goldston, B. Grek, R. J. Hawryluk, K. W. Hill, H. Hsuan, D. W. Johnson, D. C. McCune, D. M. Meade, D. Müller, D. K. Owens, H. Park, A. T. Ramsey, M. N. Rosenbluth, J. Schivell, G. L. Schmidt, S. D. Scott, G. Taylor, and R. M. Wieland, in *Plasma Physics and Controlled Nuclear Fusion Research, 1990*, Proceedings of the 13th International Conference, Washington, DC (International Atomic Energy Agency, Vienna, 1991), Vol. I, p. 109.

[13]M. Kotschenreuther, H. L. Berk, R. Denton, S. Hamaguchi, W. Horton, C.-B. Kim, M. Lebrun, P. Lyster, S. Mahajan, W. H. Miner, P. J. Morrison, D. W. Ross, R. D. Sydora, T. Tajima, J. B. Taylor, P. M. Valanzu, H. V. Wong, S. Y. Xiao, and Y. Z. Zhang, in Ref. 12, Vol. II, p. 361.

[14]G. W. Hammett and F. W. Perkins, Phys. Rev. Lett. **64**, 3019 (1990).

[15]F. L. Hinton and W. Horton, Phys. Fluids **14**, 116 (1971).

[16]C.-B. Kim, W. Horton, and B. G. Hong, Plasma Phys. Controlled Fusion **33**, 469 (1991).

[17]S. I. Braginskii, in *Review of Plasma Physics*, edited by M. A. Leontovich (Consultants Bureau, New York, 1965), Vol. 1, p. 205.

[18]S. Hamaguchi and W. Horton, Plasma Phys. Controlled Fusion **34**, 203 (1992).

[19]*Handbook of Mathematical Functions*, edited by M. Abramowitz and I. A. Stegun (Dover, New York, 1972), Chap. 21, p. 751.

[20]C. Flammer, *Spheroidal Wave Functions* (Stanford University Press, Stanford, CA, 1957), Chap. 3, p. 18.

[21]W. Park, D. A. Monticello, R. B. White, and A. M. M. Todd, Bull. Am. Phys. Soc. **23**, 779 (1978).

[22]H. R. Strauss, W. Park, D. A. Monticello, R. B. White, S. C. Jardin, M. S. Chance, A. M. M. Todd, and A. H. Glasser, Nucl. Fusion **20**, 628 (1980).

[23]Z. Chang, Ph.D. thesis, University of Wisconsin, Madison, 1991.